POLYMERS FOR ADVANCED TECHNOLOGIES
Polym. Adv. Technol. 2007; **18**: 771–779
Published online 29 May 2007 in Wiley InterScience (www.interscience.wiley.com) DOI: 10.1002/pat.934

PAT

Microstructure and nematic transition in thermotropic liquid crystalline fibers and their single polymer composites†

Estelle Kalfon–Cohen[1]*, Gad Marom[1], Amotz Weinberg[2], Ellen Wachtel[3], Claudio Migliaresi[4] and Alessandro Pegoretti[4]

[1]Casali Institute of Applied Chemistry, The Hebrew University of Jerusalem, Jerusalem 91904, Israel
[2]Shenkar College of Engineering and Design, Ramat-Gan 52526, Israel
[3]Chemical Research Infrastructure Unit, The Weizmann Institute of Science, Rehovot 76100, Israel
[4]Department of Materials Engineering and Industrial Technologies, University of Trento, Via Mesiano 77, Trento 38050, Italy

Received 22 February 2007; Accepted 25 March 2007

We describe a new single polymer composite (SPC) prepared from two liquid crystalline vectran fibers. Vectran M is the as-spun fiber while vectran HS is the high-strength version. A study of the morphology of the pristine materials shows that the two fibers have different crystal structures. The wide-angle X-ray diffraction (WAXD) data confirm the presence of the so-called pseudo-hexagonal (PH) unit cell in vectran M, while an orthorhombic structure is revealed in the vectran HS fibers. A transition to the nematic phase is observed by *in situ* X-ray diffraction at ~277°C for the M fibers and at ~315°C for the HS fibers. During the compaction process, the orientation of the reinforcing fibers is well maintained and the transition to a nematic phase seems to be delayed by processing at high applied pressure. Concomitantly, vectran M loses its orientation and the transition to the nematic phase disappears. Copyright © 2007 John Wiley & Sons, Ltd.

KEYWORDS: single polymer composite; liquid crystalline polymer; WAXD; nematic transition

INTRODUCTION

Thermotropic liquid crystalline behavior of some polymeric materials (TLCPs) is of considerable current interest, not only because of their potential as high-strength fibers and plastics, but also because of their unique structural order in fluid phases. The inherent mechanical properties are due to the high degree of alignment arising from the anisotropic shape of the monomer units, or mesogens. The extended and rigid backbone leads to axial alignment of the mesogens in the liquid crystalline phase.[1,2] Although TLCPs are of an extended chain nature, they possess characteristics that are common to amorphous and semicrystalline polymeric materials such as a rubber–glass transition and sub-glass relaxations. Wide-angle X-ray diffraction (WAXD)[3–8] studies on copolyester TLCPs indicate that the degree of orientation can be very high along the flow/processing direction.

TLCPs generally exhibit at least two phase transitions as a function of temperature. A narrow melting endotherm occurs in the temperature range between the solid crystalline and the isotropic liquid states.[9] In the discussion below we will consider melting as the crystalline to nematic transition. The anisotropic properties of a TLCP melt are similar to those of a solid, except that the molecules are free to move like common liquids. According to the Flory theory of polymeric solutions published in 1956,[10] polymers that exhibit liquid crystallinity typically consist of comparatively elongated rigid-rod molecules, and a mesophase is formed when their concentration reaches a certain level. The processing of molten TLC polymers in an elongated flow field, in spinning or in extrusion processes, results in a highly oriented and extended chain structure in the solid state. High-performance polymers such as vectra or xydar are produced from a nematic melt.[11,12] They provide good reinforcement for thermoplastic polymers and in blends.[13,14] The vectran fibers used in this study are obtained from the standard vectra polymer for injection molding. In fact, vectra polymer is subjected to specific spinning ratios and annealing conditions in order to form vectran M and the high-strength vectran HS.[15] In particular, vectran M are as-spun fibers while vectran HS fibers have been subjected to a proprietary heat treatment under tension.[15] X-ray studies of the vectra

*Correspondence to: E. Kalfon-Cohen, Casali Institute of Applied Chemistry, The Hebrew University of Jerusalem, Jerusalem 91904, Israel.
E-mail: estelle@pob.huji.ac.il
Contract/grant sponsor: Israel Science Foundation; contract/grant number: 69/05.
†This paper is presented as part of a special issue in memory of Professor Yair Avny.

polymer have revealed both pseudo-hexagonal (PH) and orthorhombic structures, depending on the annealing conditions.[16–18]

In recent studies by two of the present authors, single polymer composites (SPCs) were prepared by using two TLCP vectran fibers which are similar in their chemical composition but have markedly different physical properties.[19,20] The composite preparation was based on the preferred melting of one fiber type to generate the continuous phase of the composite (the matrix) while the second fiber type remained intact. We expected that an oriented matrix phase would be obtained upon cooling the nematic anisotropic melt to room temperature. In those reports, sample preparation and mechanical properties were studied. In this paper, the morphology of the pristine fibers and their SPCs are investigated. The characterization of the structure and morphology of these materials was based on experimental work at European Synchrotron Radiation Facility—beamline ID-11 (ESRF), where the static samples were exposed to intense X-ray microbeam radiation. The crystalline structure of the matrix, the fiber, and the interface region can be studied by focusing the beam on each region. Transitions to the liquid crystalline phase were revealed by diffraction measurements made during *in situ* heating.

EXPERIMENTAL

Materials

Two thermotropic liquid crystalline polymer fibers were selected for the sample preparation, namely a Vectran® M and a Vectran® HS fiber. Both are commercialized by Celanese Advanced Materials Inc. (Now Kuraray America Inc.) and consist of a co-polyester of 1,4 hydroxybenzoate (HBA) and 2,6 hydroxynaphtanoate (HNA) with a monomer ratio of 73/27 for HBA and HNA, respectively.[21] The random copolymerization of HNA and HBA disrupts the registry between the adjacent chains. The HNA monomer has a larger transverse size that increases the inter-chain distance, dramatically lowering the melting temperature.

Vectran M has a T_g of 113°C and a nominal melting temperature T_m of 276°C. Vectran HS has a nominal T_m of 330°C.[22] Physical and mechanical properties of each fiber are reported in Tables 1 and 2 in Reference [19]. The molecular similarity combined with different physical and mechanical behavior makes possible the preparation of SPCs. Particularly the gap between the melting temperatures of the two vectran fibers allows a working temperature window within which only the vectran M fiber can melt and form a continuous phase while the HS fiber remains intact. The composite preparation was as described in Pegoretti *et al*.[19] The two fibers were co-wound on a flat mandrel in order to obtain a composite performs with a 50\ vol% content of both type of fibers. This preform was then subjected to heating to the compaction temperature under constant pressure (1.8 MPa), where the compaction temperature may vary between 260 to 285°C. At this temperature the pressure was increased to 4.4 MPa for a few seconds following which the sample was rapidly cooled under pressure (1.8 MPa) to room temperature. The same procedure was applied to a second type of sample, for which the compaction temperature was fixed at 275°C while the compaction pressure was varied within the range of 1.8 to 8.8 MPa. Nine different types of samples were obtained with at least six specimens of each.

Table 1. Observed *d* spacings for vectran M and vectran HS fibers

Sample	Spacing *d* (Å)	Assignment
Vectran M	4.48	110
	3.25	211
	6.73	Meridional 1
	3.06	Meridional 2
	2.07	Meridional 3
Vectran HS	4.57	110
	3.96	200
	3.21	211
	6.73	Meridional 1
	3.01	Meridional 2
	2.07	Meridional 3

Polarized optical microscopy and ESEM

Visual examination of the pristine fibers and the composites was achieved with a Nikon optical microscope (POM) equipped with crossed polarizers. The transition to the mesophase was detected by using a hot stage connected to the POM. An environmental scanning electron microscope (ESEM-QUANTA 200 FEI) operating at 10 kV and under low vacuum was used to define the microstructure of the composites.

In situ WAXD measurements

Synchrotron microbeam WAXD measurements were performed at the ESRF on the Materials Science Beamline (ID-11). The X-ray microbeam was monochromatized at a wavelength of $\lambda = 0.5436$ Å and collimated to dimensions 2 μm (vertical) by 50 μm (horizontal). The exposure time for each sample varied from 10 to 20 sec. Samples were inserted into 0.5 or 1 mm diameter Li-glass capillaries (with the sample long axis parallel to that of the capillary) and mounted in a hot stage (Linkam Scientific Instruments, THMS600, Waterfield, UK). The distance between the sample and the detector was set at approximately 143 mm. Each sample was scanned during heating at 10°C/min from 25 to 500°C. Data were taken either at 5 or 10°C intervals. The one-dimensional diffraction profiles were calculated from the two-dimensional X-ray diffraction patterns using the image analysis programs Fit2D (ESRF, Dr Hammersley) and Polar (SUNY, Stony Brook, NY). The orientational distributions were determined by calculating azimuthal histograms using the d_{110} reflection from the two-dimensional patterns. The degree of orientation in liquid crystals can be described by an orientational order parameter *S* defined as.[23]

$$S = 0.5\left\langle (3\cos^2\theta) - 1 \right\rangle \quad (1)$$

where θ is the angle between the molecular axis and the director (Fig. 2), and the brackets denote an average value for many molecules.[23,24] For perfectly oriented molecules ($\theta = 0$), *S* equals to 1. The value of *S* for liquid crystalline polymers lies between 0.3 and 0.8 and decreases as the temperature is increased.[24]

DOI: 10.1002/pat

X-ray diffractometry

X-ray diffraction patterns of pristine vectran fibers were measured using a D-Max/B theta-2theta powder diffractometer (Rigaku, Japan) in conjuction with an RU200 rotating anode X-ray generator (Rigaku) with copper target. The X-radiation was monochromatized with a graphite monochrometer to an average wavelength of $\lambda = 1.54$ Å. The fibers were held vertical and the scan was made in the horizontal plane.

Calorimetry

Differential scanning calorimetry (DSC) was carried out in a Mettler DSC-30 calorimeter, at a heating rate of 10°C/min, under a nitrogen flux of 50 ml/min. The weight of each sample was about 10–15 mg.

RESULTS AND DISCUSSION

The pristine fibers

Calorimetry and polarized light microscopy

The DSC thermograms of vectran M and vectran HS are reported in Fig. 1, in which the markedly different thermal behavior of the two fibers should be clear. One distinct endotherm is observed for the HS fiber at ~315°C while for the M fiber we observed two broad endotherms at 275°C (comparable to the literature value of 276°C[21,22]) and at 290°C. The interpretation of this thermal behavior can be aided by observing one of the M type fibers with a polarized light optical microscope which is a well accepted technique for determining the nematic structure in TLCP.[25] At temperatures approaching the ''literature'' melting point no optical activity was observed as shown in Fig. 2(a). Continued heating to 277°C reveals a transition to a liquid crystalline structure as shown in Fig. 2(b) which disappears at 290°C (see Fig. 2c). The texture of the mesophase observed here can be identified as a nematic liquid crystalline phase in which the mesogens are aligned parallel to the director[25] but which have no lateral order. The two endotherms observed during heating of the M fibers can therefore be assigned to the mesomorphic transition to the nematic phase and to the transition to the isotropic phase.

Crystallography

Structural analysis of the pristine fibers using WAXD reveals that the molecular organization in these fibers is that of a polymer with a low degree of crystallinity and a high degree of orientation. X-ray diffraction patterns of the M type fibers are presented in Fig. 3(a). By comparing these data with results obtained previously with vectra sheet,[17] the crystal structure of the vectran fibers can be understood. The d spacing values calculated for the pristine fibers are presented in Table 1. Three well-defined meridional maxima at $d \approx 6.73$ Å, $d \approx 3.06$ Å, and $d \approx 2.07$ Å are observed and designated m_1, m_2, and m_3, respectively. One intense and broad equatorial reflection is observed at $d \approx 4.48$ Å and an off-equatorial maximum at $d \approx 3.25$ Å. Taken together, these last two reflections reveal the presence of some three-dimensional order and are arc shaped due to the imperfect orientation. The angular breadth of the equatorial reflection suggests an irregular lateral packing.[6] These data are compatible with the presence of the so-called PH crystalline structure in vectran M fibers, as was also found for an annealed vectra film,[5] and is characterized by the very intense equatorial reflection which is indexed as (110) and the single off-equatorial reflection indexed as (211). The non periodic nature of the meridional maxima observed in the X-ray patterns does not permit their indexing.[26,27] A similar X-ray diffraction pattern is revealed for vectran HS as presented in Fig. 3(b). The discernable splitting of the (110) reflection into two maxima indexed as (110) and (200), indicates that an orthorhombic rather than a PH unit cell is the basis of the crystalline structure of the HS fibers.[5] We know from previous studies[17] that annealing improves the lateral packing of the molecular chains resulting in the appearance of additional reflections on the equator such as (210), (200). The lattice parameters calculated for the M and the HS fiber are $a = 8.85$ and 8.37 Å, respectively and $b = 5.45$ Å. The ratio of the a and b parameters for the M fiber approaches the value of $\sqrt{3}$, which characterizes the hexagonal unit cell.[16] The c axis can not be assigned because of the non periodicity along the longitudinal axis.

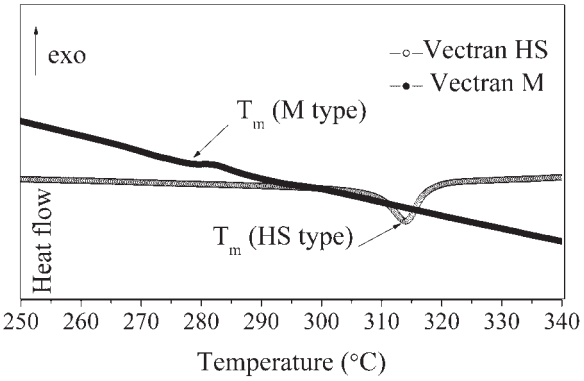

Figure 1. DSC traces of vectran M and vectran HS.

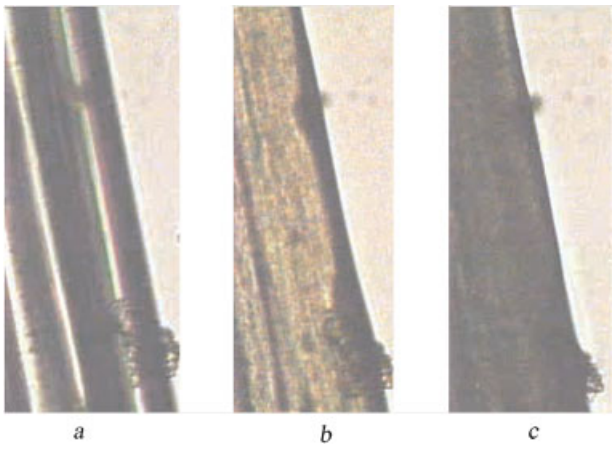

Figure 2. Polarized light micrograph taken in the orthogonal view of two vectran M fibrils at (a) 270°C, (b) 277°C, and (c) 295°C. This figure is available in colour online at www.interscience.wiley.com/journal/pat

Structure of the nematic phase

Thermal data, such as those presented in Fig. 1, can be correlated with *in situ* WAXD performed at the same heating rate (10°C/min). Figure 4 shows histograms of the azimuth-

DOI: 10.1002/pat

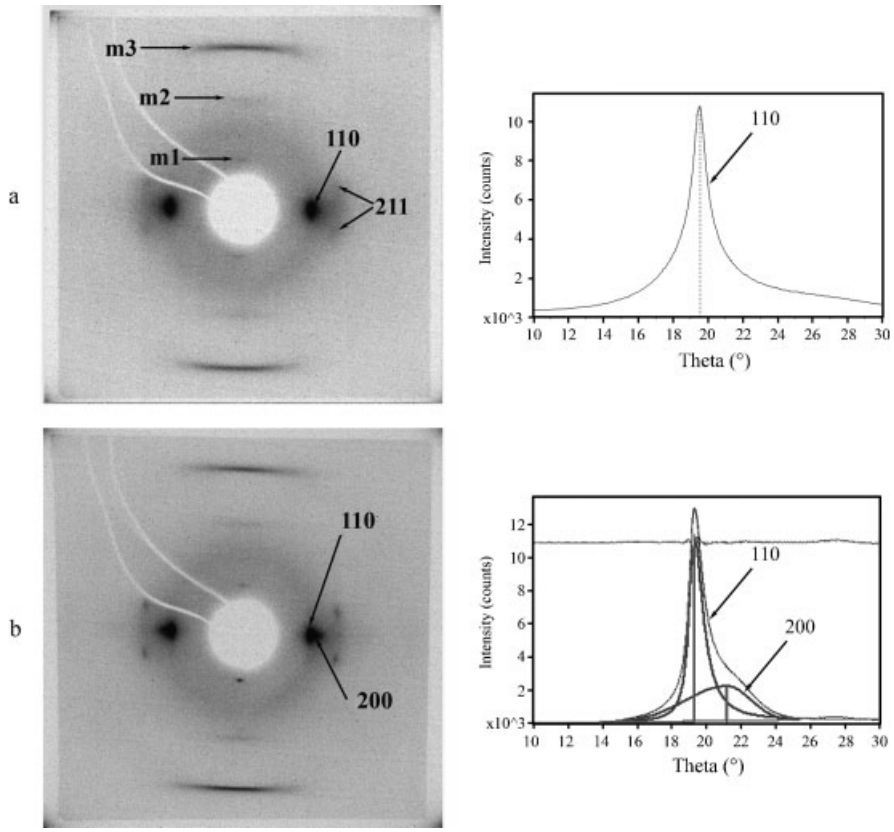

Figure 3. WAXD fiber pattern of vectran M (a) and vectran HS (b). On the right, a curve fitting of the equatorial XRD profiles.

ally averaged X-ray intensity of the vectran M at six temperatures. Upon heating the M fibers from room temperature to the isotropic phase, several features are observed. In general, at least five diffraction maxima are observed at room temperature (see Fig. 3a), and, in particular, the strong and sharp (110) reflection. Figure 4 shows that at 275°C the main reflections diminish in intensity, indicating a melting transition followed by the reappearance at 285°C of two intense diffraction maxima of the nematic structure at $d \approx 4.63$ Å and $d \approx 2.09$ Å, disappearing altogether at 295°C. The breadth of the first peak, which is associated with the lateral packing of the fiber, is consistent with the appearance of a nematic structure at temperatures approaching the melting point. The increase in diffraction intensity in the nematic phase relative to the crystalline may indicate a reorganization of the pre-melting amorphous phase into the nematic structure. The nematic transition observed in DSC at 277°C is followed by the transition to the isotropic phase at about 290°C, where only diffraction rings are visible in the X-ray pattern. The increase in d_{110} spacing values upon heating (from 4.48 to 4.63 Å) reflects the thermal expansion in the inter-chain packing involved in forming the nematic texture. In Fig. 5, the azimuthally averaged data from HS fibers at 310°C show one strong and diffuse peak at $d \approx 4.83$ Å and a weaker peak at $d \approx 2.09$ Å, consistent with the appearance of the nematic structure. The mesophase

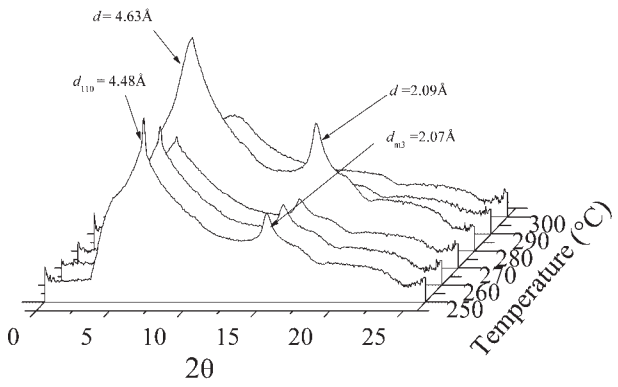

Figure 4. Histograms of the azimuthally averaged X-ray intensity of the M fibers at six selected temperatures.

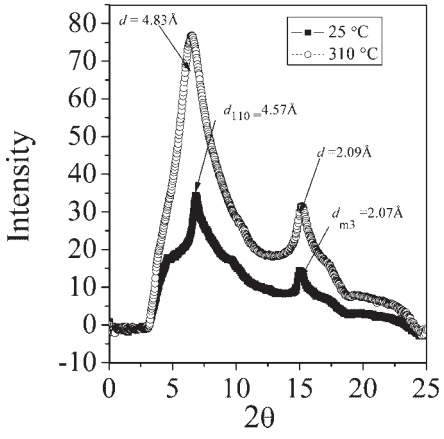

Figure 5. Azimuthally averaged X-ray intensity of vectran HS obtained in the crystalline and in the nematic state (310°C). The *d* spacings of the sharper peaks are indicated.

DOI: 10.1002/pat

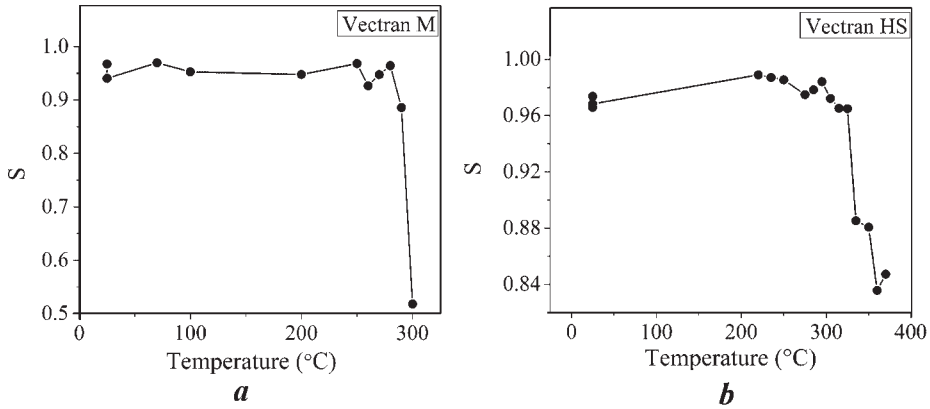

Figure 6. Effect of heating on the order parameter calculated for (a) vectran M and (b) vectran HS.

disappears upon heating to 400°C to form the isotropic liquid.

Figure 6 shows the values of the order parameter (S) obtained during heating to the melt for the M and HS fibers. Values of S higher than 0.85 are noted between 275 and 295°C in the M type fiber and above 0.80 when the HS fiber is heated to 350°C (data were taken only up to 380°C). These results reveal an oriented phase in both fibers above the melting point reported in the literature. From these results we might anticipate that preparing samples at compaction temperatures in which the M fiber shows a nematic phase will ensure an oriented continuous phase in the composite materials.

The composites

Visual inspection

Figure 7 shows scanning electron micrographs of unpolished cross-sectional cuts of vectran M/vectran HS composites. Examination reveals voids and poor interfacial adhesion within samples prepared at 260°C, 4.4 MPa (Fig. 7a) in comparison to samples prepared at 285°C, 4.4 MPa (Fig. 7b). Obviously, when the compaction temperature is raised to 275°C the vectran M fibers can flow and form a continuous phase, which acts as a binding agent within the composite. The contribution of the compaction pressure is qualitatively evaluated in Fig. 7c. A good compaction is achieved at higher pressures such as 8.8 MPa, 275°C, which allows the vectran M melt to flow and to ensure the best impregnation. In each composite sample the HS fibers remain intact and act as a reinforcing phase.

Calorimetry

Two endothermic peaks are revealed in the DSC traces obtained for composite samples as shown in Fig. 8. When the compaction temperature is 260°C and the pressure is 4.4 MPa, a low enthalpy endotherm is observed at ~280°C. Increasing the compaction temperature from 260 to 285°C (in both cases the pressure remains at 4.4 MPa) leads to a displacement of the peak by more than 12°C to higher temperatures. Conversely, the enthalpy is reduced when the preparation temperature is increased. The second endotherm observed in the DSC traces occurs at ~313°C. This

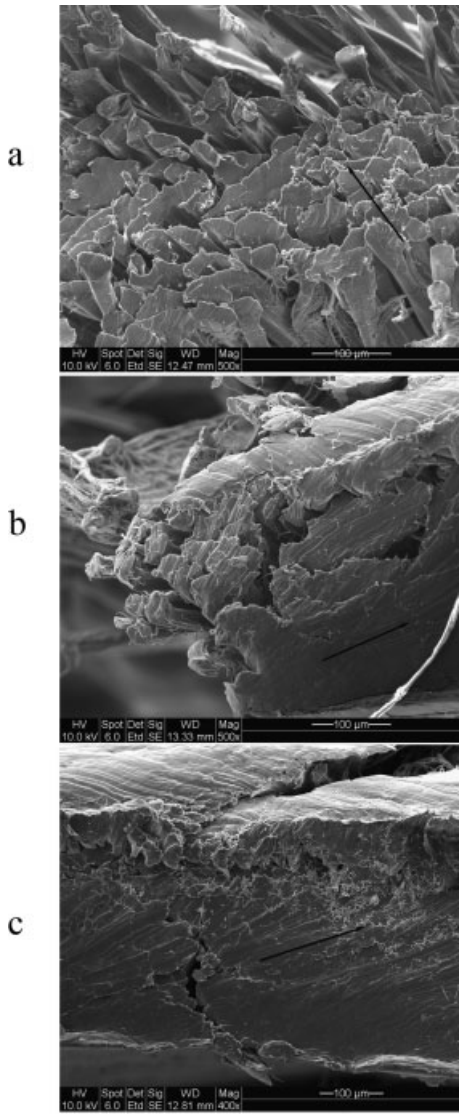

Figure 7. Scanning electron micrographs of unpolished cross-sectional cuts of composites prepared at (a) 260°C, 4.4 MPa; (b) 285°C, 4.4 MPa; and (c) 275°C, 8.8 MPa. The arrows show the cutting direction.

DOI: 10.1002/pat

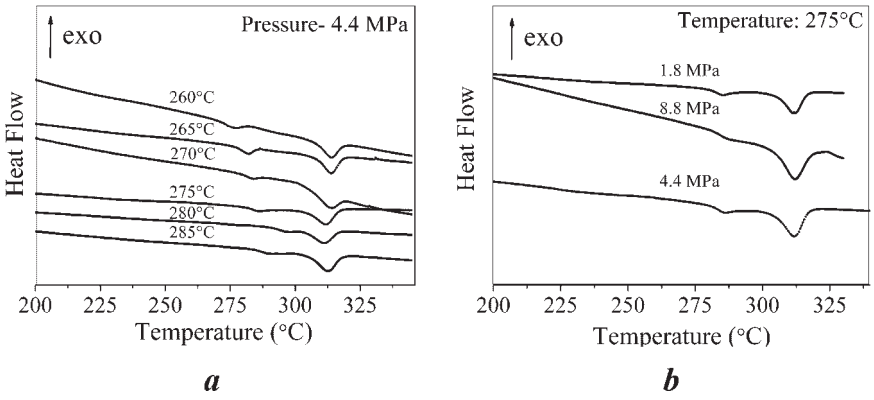

Figure 8. DSC traces of composite materials prepared at (a) different pressures and (b) different temperatures.

temperature is not influenced by either compaction temperature or pressure as seen in the results presented in Fig. 8. In view of the thermograms of the pristine fibers (Fig. 1), it is possible that the first peak at ~280°C should be assigned to a melting transition in the M fiber matrix. In this case, the very small enthalpy of the endotherm would be consistent with a very small crystalline fraction being present in the matrix of the composite prepared under these conditions of pressure and temperature. Similarly, the second endotherm would be assigned to the melting of the HS crystalline phase. Nevertheless, as will be seen below, a precise interpretation of these two endotherms requires crystallographic analysis.

Crystallography

Figure 9 shows typical room temperature X-ray diffraction patterns of the M and the HS components of a composite prepared at 275°C and 4.4 MPa. When the X-ray microbeam was focused on the M phase (Fig. 9a), two arc-shaped reflections are revealed on and near the equator indexed as the (110) and (211) of the orthorhombic unit cell, respectively. A third arc-shaped reflection is observed on the meridian and is labeled as m_3 in comparison to the pristine fiber. When the X-ray microbeam is focused on the HS fiber (Fig. 9b), the same diffraction peaks are observed as those found for the pristine HS fiber (Fig. 3b): the (110), (200), and (211) reflections on and near the equator, together with three reflections on the meridian. The strong and sharp peaks obtained on the meridian reveal a well-oriented structure similar to that observed for the pristine vectran HS. The *d* spacings calculated on the basis of Fig. 9(a) and (b) are presented in Tables 2a and 2b. Those for (110) show an increase from 4.48 Å in the pristine M fibers to 4.57 Å in samples compacted at 8.8 MPa, 275°C and from 4.57 Å for pristine HS fibers to 4.62 Å in samples compacted at 8.8 MPa, 275°C with a resolution limit of 0.02 Å.

It should be noted that no distinct interfacial structure between the fiber and the matrix is observed.

Phase transition

By focusing the microbeam on a specific phase, a structure–temperature relationship can be derived by calculating, for each pattern, the azimuthally averaged diffraction intensity. Figure 10(a) and (b) presents the histograms of the average intensity as a function of the scattering angle 2θ obtained during heating to the melt at 10°C/min, when the microbeam was focused on the matrix. The composites were prepared either at 260 or at 285°C under 4.4 MPa pressure and the results are similar. At room temperature, Fig. 10(a) shows

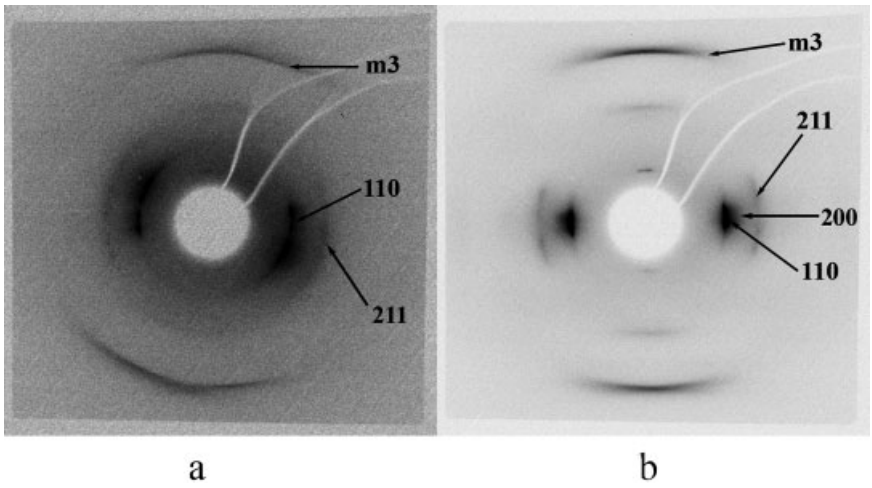

Figure 9. Typical X-ray diffraction patterns of (a) the matrix M phase and (b) the reinforcing HS fibers obtained at room temperature within composite material prepared at 275°C and 4.4 MPa.

DOI: 10.1002/pat

Table 2a. Observed *d* spacings for vectran M as the matrix component of the composite prepared at different temperatures and pressures

	Spacing *d* (Å)[a]				
Sample	110	211	Meridional 1	Meridional 2	Meridional 3
285°C, 4.4 MPa	4.52	***	***	***	2.05
275°C, 4.4 MPa	4.54	***	***	***	2.05
260°C, 4.4 MPa	4.58	***	***	***	2.06
8.8 MPa, 275°C	4.57	***	***	***	2.09
1.8 MPa, 275°C	4.55	***	***	***	2.04
M (pristine)	4.48	3.25	6.73	3.06	2.07

The results were obtained at room temperature.
[a] With a resolution limit of 0.02 Å.
*** Not observed.

Table 2b. Observed *d* spacings for vectran HS as the reinforcing component of the composite prepared at different temperatures and pressures

	Spacing *d* (Å)[a]				
Sample	110	211	Meridional 1	Meridional 2	Meridional 3
285°C, 4.4 MPa	4.54	3.21	6.37	3.05	2.05
275°C, 4.4 MPa	4.59	3.22	6.31	3.06	2.07
260°C, 4.4 MPa	4.57	3.16	6.89	3.02	2.04
8.8 MPa, 275°C	4.62	3.16	6.01	3.01	2.06
1.8 MPa, 275°C	4.57	3.23	6.10	3.04	2.06
HS (pristine)	4.57	3.21	6.73	3.01	2.07

The results were obtained at room temperature.
[a] With a resolution limit of 0.02 Å.

two weak crystalline peaks which are identified as the (110) and m3 reflections. The high baseline of the histogram indicates a large amorphous component present in the matrix. The two reflections disappear upon heating to 250°C and are replaced by diffuse peaks (halos) characteristic of an isotropic phase. No transition to the nematic melt is observed during heating. The same thermal behavior is observed in the sample prepared at 285°C, 4.4 MPa. In both cases, the weak intensity at room temperature of the (110) and m3 peaks reveals the very small fraction of crystalline polymer in the matrix.

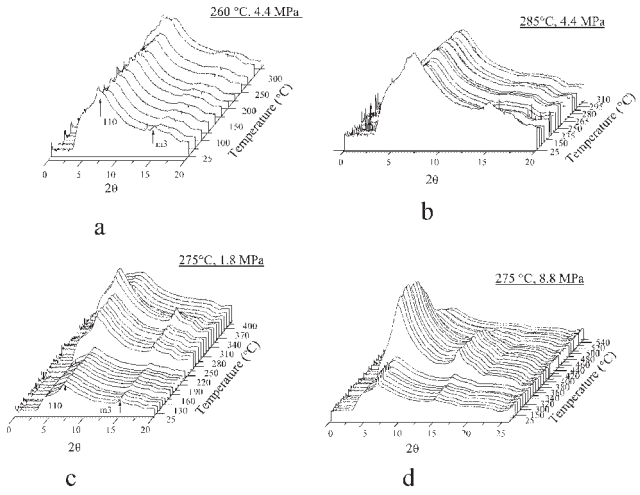

Figure 10. Histograms of the azimuthally averaged X-ray intensity as a function of temperature when the microbeam is focused on the matrix part (a) and (b), and on the reinforcing part (c) and (d) of the composite prepared at different pressure and temperature conditions.

Figure 10(c) and (d) present the resulting histograms of the average intensity during heating to the isotropic state when the microbeam was focused on the fiber. In one case the composite was prepared at 1.8 MPa, 275°C (Fig. 10c), while in the second case the conditions were 8.8 MPa, 275°C (Fig. 10d). By comparison to the WAXD pattern of the fiber in Fig. 9(b), the orthorhombic structure can be identified by the strong (110) peak on the equator at $d \approx 4.57$ and 4.62 Å for samples prepared at 1.8 and 8.8 MPa, respectively and the third meridional (m3) reflection at $d \approx 2.06$ Å in the fiber phase under the two compaction conditions. When the samples are heated, the following features are observed. In Fig. 10(c), a first increase in intensity in the vicinity of these two reflections is observed at ~270°C. This transition is followed by a second increase in intensity upon heating to 320°C which seems to indicate a second stage in the transition to the nematic phase. At and above 380°C, only weak, diffuse diffraction rings are observed, consistent with a transition to the isotropic phase.

In Fig. 10(d), crystalline peaks are observed from room temperature until 320°C. Above this temperature the increased breadth and intensity of the diffraction peaks indicate a transition occurring in the crystalline phase. Therefore, the transition to the nematic state occurs at ~320°C with the disappearance of the crystalline peaks and the increase in the intensity at ~350°C. This phase remains stable from 350 to 480°C. At higher temperatures the isotropic phase is observed. It should be noted that the nematic transition is retained over a larger temperature

DOI: 10.1002/pat

range when the pressure applied during the compaction is increased.

It is now possible to discuss the correlation between the calorimetry and the X-ray diffraction results for the vectran M/vectran HS composites (it should be noted that calorimetry determines the transition midpoint whereas with WAXD, the transition endpoint is identified).

In the thermograms in Fig. 8(a) and (b), two endotherms were observed: a very low enthalpy peak at ~280°C and a second significantly stronger endotherm at ~313°C. The small fraction of the chains in the crystalline state present in the matrix, as reflected in the weak intensity of the crystalline peaks at room temperature (Fig. 10a and b), is responsible for the low enthalpy of the peak at ~280°C. This transition is hardly observed in the WAXD histograms obtained when the microbeam was focused on the matrix (Fig. 10a and b), because of its very low enthalpy. In this case, we can assign the endotherm at 280°C to a transition in which the vectran M matrix transforms directly from the weak crystalline to the isotropic phase. Accordingly, the second endotherm then reflects the strong transition to the nematic state observed in the WAXD histograms of the fiber in Fig. 10(c) and (d). It should be noted from Fig. 10(c) that the intensity is observed to increase in two stages, at ~270 and ~320°C. In this case, the first endotherm observed in Fig. 8(b) corresponds to both: the melting of the matrix and the first stage of the nematic transition in the fiber. The second endotherm then corresponds to the second and stronger nematic transition in the fiber observed in the WAXD histogram. The unique transition observed in Fig. 10(d) reflects the second endotherm observed in Fig. 8(b) at ~313°C.

The transition from the crystalline to the nematic state together with the transition from the nematic to the isotropic state may also be characterized by calculating the orientational order parameter *S* during heating, as shown in Fig. 11. For the sample prepared at 8.8 MPa, three well-defined regions are observed. High orientational order is observed from 25 to ~350°C, the nematic liquid crystalline phase with intermediate orientational order is seen between ~350 and ~480°C and the isotropic liquid above 480°C.

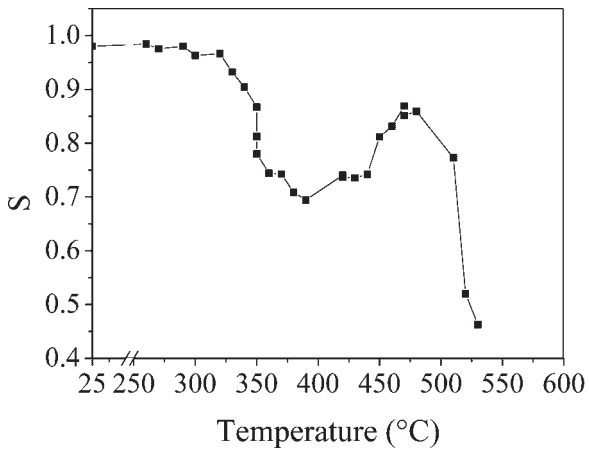

Figure 11. Effect of heating on the order parameter calculated from the HS reinforcing fiber within the composite prepared at 275°C, 8.8 MPa.

CONCLUSIONS

Crystallographic parameters for vectran M and HS fibers are derived for the first time from X-ray analysis. An orthorhombic structure is predominant in the HS fiber, while a PH crystalline phase characterizes the M fiber. A transition to a nematic liquid crystalline mesophase is observed in both fibers at temperatures near the melting point as reported in the literature. In the M/HS composites a similar microstructure is revealed; the reinforcing component (HS) and, to a more limited extent, the continuous phase (M), retain a high degree of orientation. The orthorhombic structure is retained in the reinforcing phase. The X-ray diffraction patterns acquired during heating show a nematic transition only in the HS component which is shifted and retained to higher temperatures with compaction pressure.

Acknowledgments

This research was supported by the Israel Science Foundation (grant no. 69/05). The authors are indebted to L. Gilat for her assistance in the interpretation of the synchrotron measurements.

REFERENCES

1. Chae HG, Kumar S. Rigid-rod polymeric fibers. *J. Appl. Polym. Sci.* 2005; **100**: 791–801.
2. Chung TS. The recent developments of thermotropic liquid crystalline polymers. *Polym. Eng. Sci.* 1986; **26**: 901–919.
3. Gutierrez GA, Chivers RA, Blackwell J, Stamatoff JB, Yoon H. The structure of liquid crystalline aromatic copolyesters prepared from 4-hydroxybenzoic acid and 2-hydroxy-6naphtanoic acid. *Polymer* 1983; **24**: 937–942.
4. Blackwell J, Biswas A, Gutierrez GA, Chivers RA. X-ray analysis of the structure of liquid crystalline copolyester. *Faraday Discuss. Chem. Soc.* 1985; **79**: 73–84.
5. Wilson DJ, Vonk CG, Windle AH. Diffraction measurements of crystalline morphology in a thermotropic random copolymer. *Polymer* 1993; **34**: 227–237.
6. Langelaan HC, Posthuma de Boert A. Crystallization of thermotropic liquid crystalline HBA/HNA copolymers. *Polymer* 1996; **37**: 5667–5680.
7. Biswas A, Blackwell J. Three dimensional structure of main chain liquid crystalline copolymers. 2. Interchains interference effects. *Macromolecules* 1988; **21**: 3152–3158.
8. Hudson SD, Lovinger AJ. Transmission electron microscopic investigation of the morphology of a poly(hydroxybenzoate-co-hydroxynaphthoate) liquid crystal polymer. *Polymer* 1993; **34**: 1123–1129.
9. Collings PJ. *Liquid Crystals: Nature's Delicate Phase of Matter*. Adam Hilger: Bristol, 1990.
10. Flory PJ. Phase equilibriums in solutions of rodlike particles. *Proc. Roy. Soc.* 1956; **234A**: 73–89.
11. Yoon HN, Charbonneau LF, Calundann GW. Synthesis, processing and properties of thermotropic liquid-crystal polymers. *Adv. Mater.* 1992; **4**: 206–214.
12. He X, Ellison MS, Paradkar RP. Spinnability and physical properties of in situ composite fibers based on thermotropic liquid crystalline polymer. *J. Appl. Polym. Sci.* 2002; **86**: 795–811.
13. Machiels AGC, Denys KFJ, Van Dam J, De Boer AP. Effect of processing history on the morphology and properties of polypropylene/thermotropic liquid crystalline polymer blends. *Polym. Eng. Sci.* 1997; **37**: 59–72.
14. Kim SH, Lim DK, Yi SC, Oh KW. Thermotropic liquid crystal polymer fabric reinforced polyimide composite materials. *Polym. Comp.* 2000; **21**: 806–813.
15. Taylor JE, Romo-Uribe A, Libera MR. Molecular orientation gradients in thermoplasticliquid crystalline fiber. *Polym. Adv. Technol.* 2003; **14**: 595–600.
16. Sun Z, Cheng HM, Blackwell J. Structure of annealed copoly (p-hydroxybenzoic acid-2-hydroxy-6-naphtanoic acid). 1. Chain conformation and packing. *Macromolecules* 1991; **24**: 4162–4167.

DOI: 10.1002/pat

17. Kaito A, Kyotani M, Nakayama K. Effects of annealing on the structure formation in thermotropic liquid crystalline copolyester. *Macromolecules* 1990; **23**: 1035–1040.
18. Kim YC, Economy J. The degradation process observed during step annealing of 73/27 HBA/HNA. *Macromolecules* 1999; **32**: 2855–2860.
19. Pegoretti A, Zanolli A, Migliaresi C. Preparation and tensile mechanical properties of unidirectional liquid crystalline single-polymer composites. *Comp. Sci. Technol.* 2006; **66**: 1970–1975.
20. Pegoretti A, Zanolli A, Migliaresi C. Flexural and interlaminar mechanical properties of unidirectional liquid crystalline single-polymer composites. *Comp. Sci. Technol.* 2006; **66**: 1953–1962.
21. Menczel JD, Collins GL, Saw SK. Thermal analysis of Vectran® fibers and films. *J. Thermal Anal.* 1997; **49**: 201–208.
22. http://www.vectranfiber.com/general_properties.asp
23. Roe RJ. *Methods for X-ray and Neutron Scattering in Polymer Science*. Oxford University press: England, 2000.
24. Tjong SC. Structure, morphology, mechanical and thermal characteristics of the in-situ composites based on liquid crystalline polymers and thermoplastics. *Mater. Sci. Eng.* 2003; **41**: 1–60.
25. Sawyer LC, Chen RT, Jamieson MG, Musselman IH, Russell PE. The fibrillar hierarchy in liquid crystalline polymers. *J. Mater. Sci.* 1993; **28**: 225–238.
26. Blackwell J, Gutierrez GA, Chivers RA. Diffraction by aperiodic polymer chains: the structure of liquid crystalline copolyester. *Macromolecules* 1984; **17**: 1219–1224.
27. Blackwell J, Biswas A, Gutierrez GA, Chivers RA. X-ray analysis of the structure of liquid-crystalline copolyester. *Faraday Discuss. Chem. Soc.* 1985; **79**: 73–84.

DOI: 10.1002/pat